Biosensors and Bioelectronics 137 (2019) 88–95

Contents lists available at ScienceDirect

Biosensors and Bioelectronics

journal homepage: www.elsevier.com/locate/bios

Porous graphene-black phosphorus nanocomposite modified electrode for detection of leptin

Jinying Cai[a,1], Xiaodan Gou[b,1], Bolu Sun[a], Wuyan Li[c], Dai Li[a], Jinglong Liu[a], Fangdi Hu[a,*], Yingdong Li[d,**]

[a] School of Pharmacy, Lanzhou University, Lanzhou 730000, China
[b] School of Chemistry and Chemical Engineering, Nanjing University, 210046, China
[c] Center for Inflammation, Translational and Clinical Lung Research, Temple University School of Medicine, Philadelphia, PA, USA
[d] Affiliated Hospital of Gansu University of Chinese Medicine, Lanzhou 730000, China

ARTICLE INFO

Keywords:
Non-alcoholic fatty liver disease
Leptin
Electrochemical immunosensor
Porous graphene-black phosphorus
Label-free

ABSTRACT

Leptin is a vital biomarker of non-alcoholic fatty liver (NAFLD), and its evaluation of the concentration level *in vivo* is of great significance to NAFLD diagnosis. Therefore, it is pressing to develop a method for rapid and sensitive detection of leptin. This paper describes an environmentally friendly and label-free immunosensor based on porous graphene functionalized black phosphorus (PG-BP) composite to detect of leptin. The PG-BP was synthesized via strong coherent coupling between porous graphene (PG) surface plasmons and anisotropic black phosphorus (BP) localized surface plasmons, which made the electrochemical performance of PG and BP synergistic as well as increased the stability and conductive capability of BP material. The PG-BP modified electrodes was further prepared by gold nanoparticles, cysteamine, and glutaraldehyde in turn. Due to the cross-linking effect of glutaraldehyde, anti-leptin can be firmly fixed. These properties of the platform improved the conductive capability of the immunosensor and enhanced the load capacity of the proteins, thereby, the sensitivity of the immunosensor was significantly increased. Under the optimal conditions, the proposed immunosensor exhibited a wide linear range of 0.150–2500 pg/mL with a low detection limit of 0.036 pg/mL. The leptin immunosensor displayed excellent selectivity and anti-interference ability, which could be used for early screening and diagnosis of clinical NALFD.

1. Introduction

Non-alcoholic fatty liver disease (NAFLD) is a clinical pathological syndrome, which show up as fatty deposition and hepatic lobular lesions in the liver caused by other factors except for excessive drinking (Rinella and Sanyal, 2016). Thus, realizing the early screening and diagnosis of NAFLD is vital for metabolic health and prevention of multisystem diseases. Currently, those methods that are commonly used remains deficient (Alkhouri et al., 2010; Zhou et al., 2018). For instance, the liver biopsy (Byrne and Targher, 2016) is an unrealistic screening tool for large high-risk obese people due to the high risk, high cost and various other shortcomings of liver biopsy techniques, the sensitivity of routine liver function blood tests (Chalasani et al., 2012) is not enough and ultrasound examinations (Rau et al., 2015) cannot prompt the diagnosis of pathological anatomy. Above all, and with the development of biomarker research in context, it is urgent to start from the pathological mechanism of NAFLD to find a related substance *in vivo* as a diagnostic index of NAFLD, so as to construct a method that can effectively and practically detect and diagnose NAFLD.

As a vital potential biomarker of NAFLD, leptin is of great significance for the NAFLD (Jenkins et al., 1997; Pérez-Pérez et al., 2017), which was used to diagnose NAFLD based on the serum concentration in this study. To date, the detection of leptin typically rely on Radio immunoassay, Enzyme-linked immunosorbent assays, Immunofluorescence assay and so on (Kim and Son, 2016; Schmidt et al., 2016; Stannus et al., 2013; Ye et al., 2016), which have good sensitivity and specificity. However, there are some restrictions and limitations with these detection methods, such as the expensive equipment and cumbersome procedures. Therefore, the development of a convenient, efficient, sensitive and cost-effective method for leptin detection has been

* Corresponding author.
** Corresponding author.
E-mail addresses: hufd@lzu.edu.cn (F. Hu), lydj412@163.com (Y. Li).
[1] These authors contributed equally to this work.

https://doi.org/10.1016/j.bios.2019.04.045
Received 4 January 2019; Received in revised form 6 April 2019; Accepted 23 April 2019
Available online 29 April 2019
0956-5663/

brought into focus. Because the electrochemical immunosensor combines the specificity and affinity of the antibody-antigen reaction and the high sensitivity, low cost, high efficiency and portability of the electrochemical technique, it has attracted much attention in the field of clinical disease diagnosis. Sun et al., (2018), developed an electrochemical immunosensor for early screening of depression marker-heat shock protein 70 (HSP70) based on the porous graphene (PG), which with good precision, acceptable stability, excellent reproducibility and satisfactory results. However, the analysis performance of the sensor is determined by two aspects: the conductive capability of the substrate material and the immobilization of the antibody。 Therefore, the selection of substrate material having excellent conductive capability, high density and strong antibody immobilization, as well as maintaining the biological activity of the antibody is the key to improve the analytical performance of the sensor (Cho et al., 2018; Wen et al., 2017; Yáñezsedeño et al., 2017).

Black Phosphorus (BP), a new two-dimensional nanomaterial composed of puckered lattice configuration, has more excellent biocompatibility and lower toxicity comparing with other two-dimensional materials (Cho et al., 2016), and also shows unique semiconducting characteristics (Avsar et al., 2015), extremely high hole mobility, anisotropic conductance and higher surface to volume ratio (Chen et al., 2016; Gusmão et al., 2017; Rui et al., 2017; Tuteja and Neethirajan 2018). At present, some researchers have used BP in the field of sensors. For example, Chen et al. (Chen et al., 2016), used few-layer BP nanosheets labeled with gold nanoparticle-antibody conjugates to fabricate A BP-based field-effect transistor biosensor, Kumar (Kumar et al., 2016) and Carmen (Mayorga-Martinez et al., 2016) also built biosensors based on BP for the detection of different target analytes, which gave better results and expanded the application of BP. PG, with stable chemical properties, compact lattice structure and excellent conductive capability, has achieved good results in the field of sensors (Liu et al., 2018; Pang et al., 2018; Zhang et al., 2018). In this study, it was used to encapsulate BP via strong coherent coupling between graphene surface plasmons and anisotropic BP localized surface plasmons, realized by the formation of P—C bond (Liu et al. 2017a, 2017b; Nong et al., 2018). Thus, a composite material having high stability, good biocompatibility, excellent conductive capability and high surface area is obtained, which is porous graphene functionalized black phosphorus (PG-BP). These features provide excellent conditions for biometric and electronic signal transduction. In summary, the PG-BP has great potential as a substrate material for the leptin sensor.

In this study, PG-BP with stable properties, large specific surface area, and excellent conductive capability was constructed by infrared drying method. However, considering that the surface of the PG-BP material lacks an antibody binding site, the anti-leptin immobilization need to form SAMs of cysteamine onto the PG-BP modified electrode surface. Consequently, in this study, using gold nanoparticles has thiol groups bound to cysteamine surface strongly. Then, glutaraldehyde was used as a cross-linking agent that binds amine groups found on cysteamine and the other amino ends at the antibody molecules (Sonuc Karaboga et al., 2016). Due to the excellent conductive capability of the composite under natural environment and vacuum condition, it could be further used as a carbon electrode modified material to construct an immunosensor for the rapid detection of leptin in human serum sample, (Scheme 1). Therefore, the objective of our work is to provide a new, eco-friendly and economical, label-free assay for clinical testing and has potential value for clinical diagnosis of nonalcoholic fatty liver disease.

2. Material and methods

2.1. Apparatus and reagents

Electrochemical measurements were performed on a CHI 6041E workstation (Shanghai Chenhua, China). The different concentration of leptin, biotinylated leptin monoclonal antibody (biotin-ab) and hrp-labeled streptavidin (hrp-strept) were formulated using the appropriate dilutions from the kits provided by Elabscience biotechnology co., Ltd for subsequent experiments. All chemicals were analytical pure grade, and distilled water was used throughout the experiment. Each experiment was always carried out in a nitrogen atmosphere to avoid interference with substances in the air (Wang et al., 2009). For additional details please see the supplementary materials.

2.2. Materials preparation

2.2.1. Preparation of BP

Bulk BP was used for preparation of BP by ultrasonication (Tuteja and Neethirajan, 2018). 12.01 mg of bulk BP was dispersed in 200 mL of acetonitrile, while nitrogen was inlet to eliminate air to prevent BP from being oxidized. Then, it was handled for 4 h at 25 °C using a cell cracker (the program was set to work 2 s with a 2 s break in between). The supernatant was collected by centrifuging the above sonicated suspension (1500 rpm, 20 min), in order to remove the residual unexfoliated particles, and finally the BP nanosheets dissolved in acetonitrile was obtained.

2.2.2. Preparation of PG

The PG was synthesized by pyrolytic method (Sun et al., 2018). The mix of Na (2 g) and ethanol (5 mL) with a molar ratio 1 : 1 was added into stainless reactor, being heated to 220 °C and kept for 48 h. The white product mentioned above was cracked to black with deionized water. The black product was washed several times with deionized water and was lyophilized, finally PG was obtained. The PG powder was prepared as 1 mg/mL suspension (dissolved by isopropanol) for the following experiment.

2.3. Preparation of immunosensor

The surface of GCE was polished with 0.3 μm and 0.05 μm Al_2O_3 slurry, repeatedly. Subsequently, the surface was ultrasonically cleaned (59 kHz, 200 W) with ultrapure water and absolute ethanol several times until the surface of the electrode appear like a mirror. BP (3 μL) and PG (4.2 μL) were added dropwise respectively on GCE, then PG-BP/GCE was obtained by infrared drying. In the following step, firstly, PG-BP/GCE was instantly immersed in AuNPs solution and left in the dark for 24 h. Secondly, AuNPs/PG-BP/GCE was placed in the cysteamine (Cys) solution (60 mM, pure ethanol) and allowed to stand overnight in the dark. Then, for the covalent interaction between Cys on AuNPs modified PG-BP/GCE and anti-leptin, glutaraldehyde (Glu) solution of 0.1% was incubated as cross-linking agent for 15 min. Finally, the prepared electrodes were immersed into 10 μL 20 ng/mL anti-leptin solution in a dark medium for 120 min and the 10 μL 1% BSA was used to block the active sites. After each step of modification, the electrodes were washed with ultra-pure water and dried with argon gas gently.

2.4. Introduction to experimental methods

Differential pulse voltammetry (DPV), square wave voltammetry (SWV) and electrochemical impedance measurement (EIS) were used to characterize the electrode modification step. The electrochemical methods (DPV, SWV and EIS) were performed in 0.5 mM $[Fe(CN)_6]^{3-/4-}$. In addition, Since SWV is the most sensitive detection method in voltammetry, it is also applied to the section of optimization studies of the immunosensor, the analytical characteristics of the immunosensor and the real sample analysis. Chronocoulometry was used to study the electrochemical effective surface area of GCE, PG/GCE and BP-PG/GCE electrodes.

Infrared, Raman, SEM and XPS were used to analyze structural difference of the electrode surface during the manufacturing process of the immunosensor.

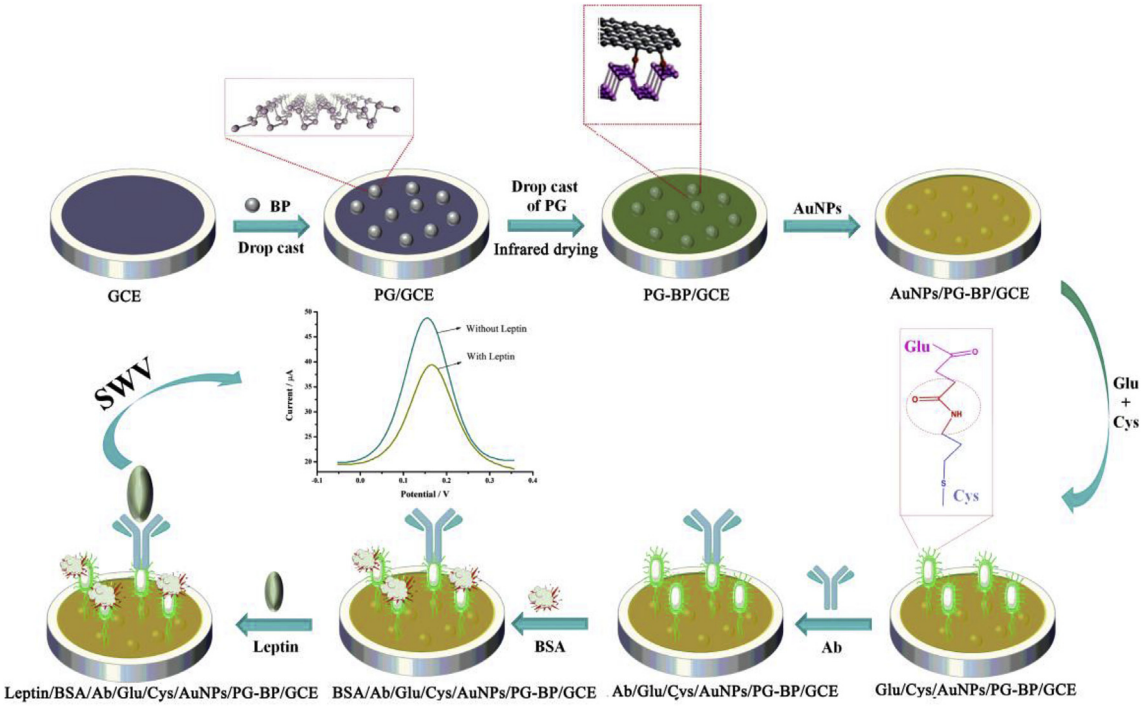

Scheme 1. Fabrication of the leptin-immunosensor.

2.5. Electrochemical detection

In this section, the target analyte was examined based on an optimization studies of the immunosensor. The immunosensor was immersed into the PBS solution (pH 7.4) with different concentrations of leptin and incubated for 2 h. Then the prepared immunosensor was rinsed with PBS and ultrapure water for twice, and air-dried (at 37 °C) in order to remove any residue and loosely bound leptin from the immunosensor surface. Finally, the immunosensor was placed into the cell containing $[Fe(CN)_6]^{3-/4-}$ solution for SWV scanning, each in triplicate. The analysis curve that related to leptin concentrations and current responses was obtained, which mentioned in section 3.5 (Fig. 3B).

3. Results and discussion

3.1. Characterization of the PG-BP

The morphologies of pure BP, PG and PG-BP were studied by field emission scanning electron microscopy (FE-SEM) and energy dispersive spectrometer (EDS). As shown in Fig. 1A, the BP presents a typical folded structure, which indicates that BP has a large specific surface area (Sajedimoghaddam et al., 2017). Fig. 1B and C represent the morphologies of PG and PG-BP, separately. Because the surface of BP was covered by PG, the combination of BP and PG cannot be observed in the vision of SEM. Therefore, this study further used EDS to investigate the elemental mapping of PG-BP material (Rui et al., 2016). As can be seen from the SEM image of PG-BP (D) and its corresponding elemental mappings of carbon (E) and phosphorus (F), PG has been successfully covered on the surface of BP.

To further confirm that BP was successfully modified with PG, Fourier transformation infrared spectroscopy (FT-IR) was used and showed in Fig. 1G. PG-BP shows four peaks appearing at 1130, 1470, 1630 and 1730 cm^{-1}, corresponding to $\nu_{\mathbf{p-0-c}}$, ν_{P-C}, $\delta_{CH_2}$and $\nu_{c=o}$, and PG just show one which corresponding to δ_{CH_2}(1630 cm^{-1}), these results proved the successful link of PG and BP. According to reports, P—C bonds will remarkably contribute to the stability of BP (Liu et al., 2017a).

Fig. 1H displayed the Raman images of BP, PG and PG-BP. In comparison to the Raman spectra of BP and PG, PG-BP shows a weak peak corresponding to P—C bonds at 813 cm^{-1} (Liu et al., 2017b). Indicating that PG-BP had been successfully synthesized, and the result was consistent with the above characterization.

The intensity of P—C bonds was further studied by X-ray photoelectron spectroscopy (XPS) (Fig. 1L). As shown in Fig. 1L, The C—O and C═O bonds are observable, which exist on the surface of PG. Furthermore, the P—C bonds were detected at ~284 ev, which implied that because of the C—O and C═O bonds increased structural disorder and reduced the energy barrier to chemical reaction, the formation of P—C bonds were promoted (Liu et al., 2017a).

3.2. Optimization studies of the immunosensor

In the optimization study of leptin immunosensor, the fixed time and other parameters of the antibody were investigated to obtain an immunosensor system with high sensitivity and good reproducibility. In addition, the immobilized ratios and the immobilized amounts of PG and BP was optimized, which was shown in Figs. 1S and 2S.

To determine the effect of anti-leptin incubation time to the immunosensor system response, Glu/Cys/AuNPs/PG-BP/GCE was incubated in anti-leptin for 30, 60, 90, 120, 150 and 180 min for determination of 625 pg/mL leptin standard solution. From Fig. 2A, the incubation time of anti-leptin greatly affected the response of the immunosensor. In the case of short incubation time, anti-leptin may not be effectively immobilized on the surface of the electrode. However, if the time is too long, the protein content on the electrode surface may be too high, so that the electrode surface would be insulated and even destroyed. Therefore, it is indicated that anti-leptin was stably immobilized on the electrode when there was no significant change of current. So 120 min was selected as the optimal incubation time of anti-leptin.

Another optimized parameter is the anti-leptin concentration to the immunosensor system response, immunosensors designed with different concentrations of anti-leptin (5, 10, 15, 20, 25 and 30 ng/mL) were used to determine 625 pg/mL leptin standard solution. As can be seen from Fig. 2B, the loading on electrode is incomplete when the

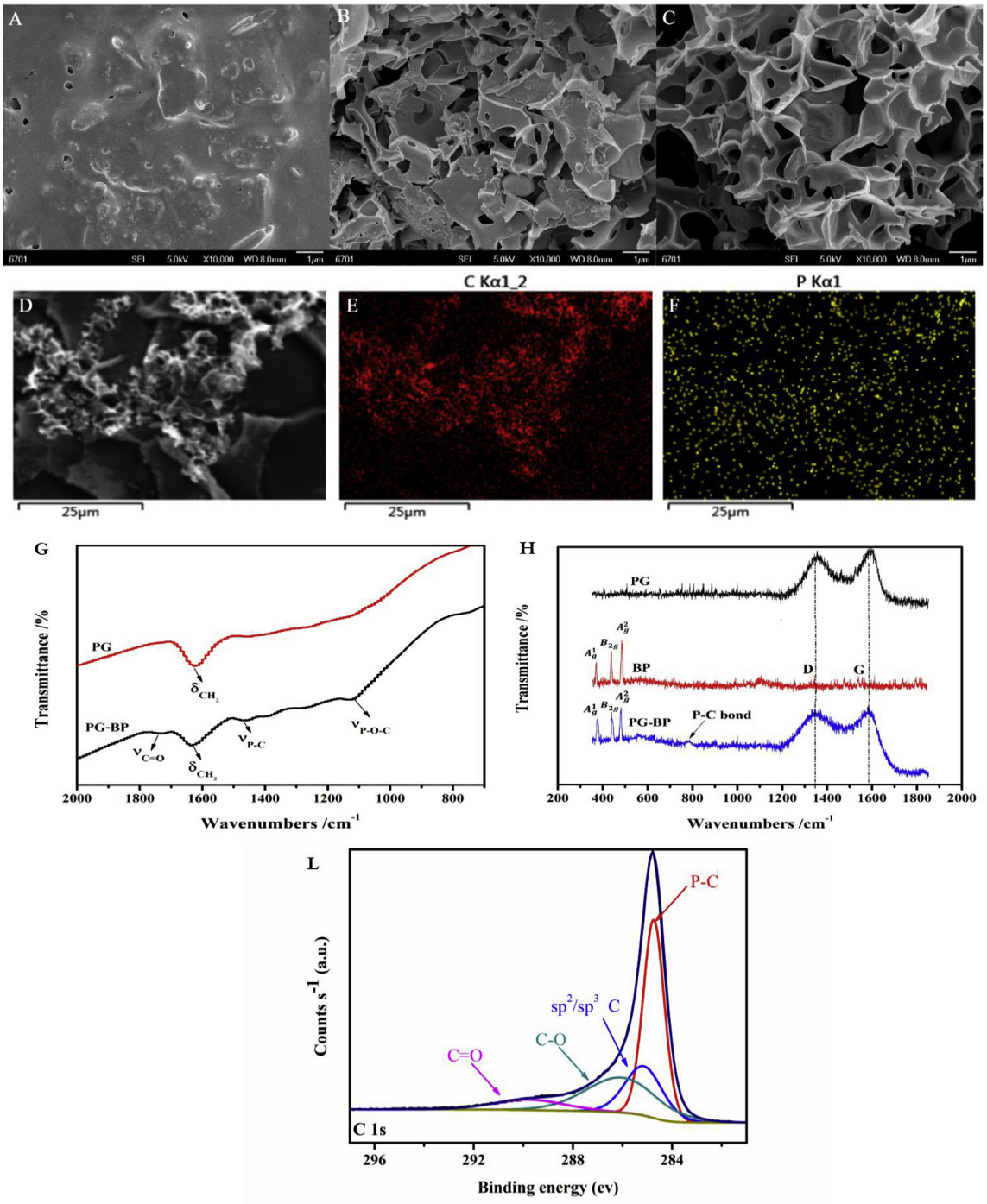

Fig. 1. The FE-SEM images of (A) BP, (B) PG and (C) PG-BP. The SEM image of PG-BP (D) and corresponding elemental mapping of the C-k line (E) and the P-k (F) line of the thin film's cross section. (G) The FT-IR spectra of PG and PG-BP, (H) the Raman spectra of PG, BP and PG-BP and (L) high resolution C 1s XPS spectrum of PG-BP.

concentration below 20 ng/mL. While the anti-leptin concentration is further increased, the electrochemical reaction would not change any more. Therefore, 20 ng/mL anti-leptin was chosen as the optimal concentration for the construction of immunosensor.

3.3. Electrochemical characterization of PG-BP/GCE

The increase of the GCE electrochemical effective area facilitates the loading of the antibody on the electrode surface and enhances the electrochemical response signal of the substance of interest. In this study, the electrochemical effective surface area of GCE, PG/GCE and BP-PG/GCE electrodes was studied using chronocoulometry (Fig. 2S). According to Anson equation (Li et al., 2018)

$$Q(t) = \frac{2nFAcD^{1/2}t^{1/2}}{\pi^{1/2}} + Q_{dl} + Q_{ads}$$

Q_{ads} is the Faradaic charge, Q_{dl} is the double layer charge, F means the Faraday constant, D means the diffusion coefficient, n represents the number of electron transfer and other parameters, such as π and t, are in their normal meaning. According to the equation, the electrochemical effective area of GCE, PG/GCE and BP-PG/GCE can be calculated as 0.016, 0.047, 0.090 cm^2, respectively. The results indicated

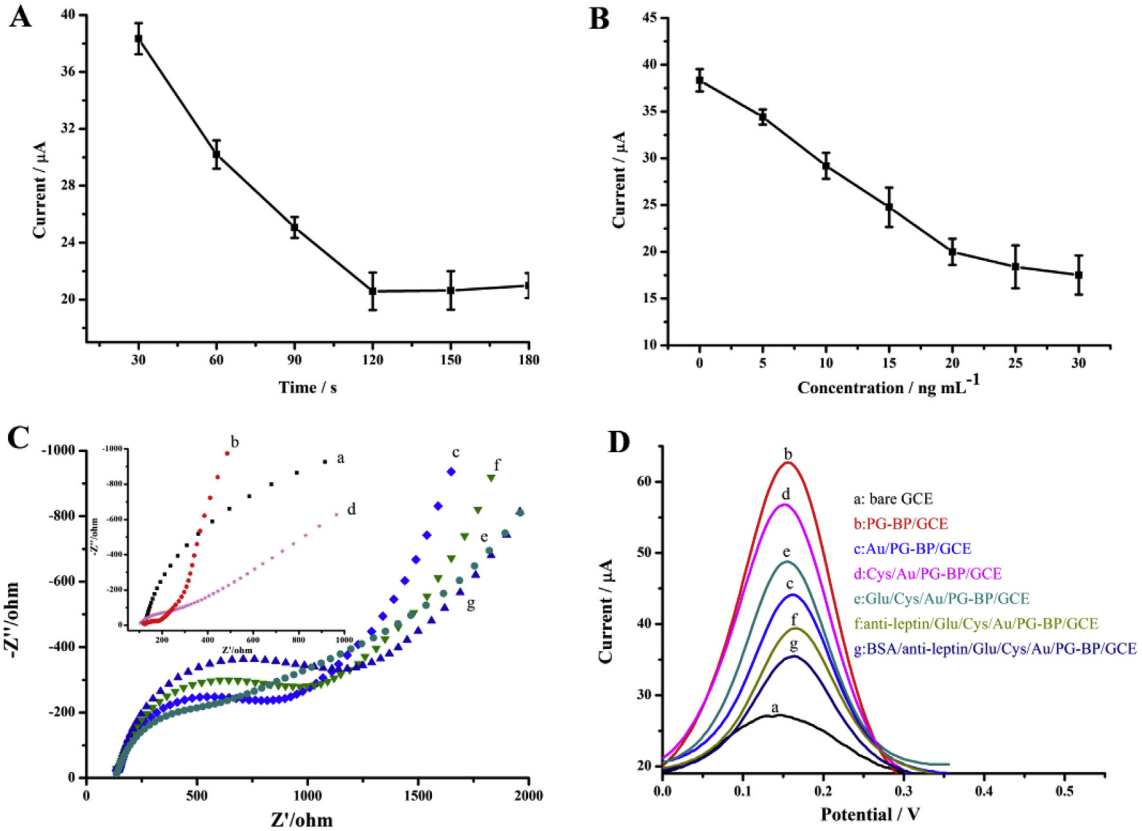

Fig. 2. (A) Effect of anti-leptin incubation time to current response on immunosensor. (B) Effect of anti-leptin concentration to current response on immunosensor. Nyquist plots (C) and SWV (D) of the different stages of the immunosensor development:(a) bare GCE, (b) PG-BP/GCE, (c) AuNPs/PG-BP/GCE, (d) Cys/AuNPs/PG-BP/GCE, (e) Glu/Cys/AuNPs/PG-BP/GCE, (f) anti-leptin/Glu/Cys/AuNPs/PG-BP/GCE, (g) and BSA/anti-leptin/Glu/Cys/AuNPs/PG-BP/GCE. Measurements were performed in 0.5 mM $[Fe(CN)_6]^{3-/4-}$ solution in 0.1 M PBS (pH = 7.4) applying a frequency range from 10^{-1} to 10^{5} Hz with an amplitude perturbation of 5 mV.

that the surface area of the electrochemical sensor was greatly increased by PG-BP.

Moreover, cyclic voltammetry was applied to scan the same decorated PG-BP/GCE 50 times in a row (Fig. 3S), the measured oxidation peak current was 90.1% of the initial detection value, which demonstrates that BP has shown good stability in this study after being functionalized by PG.

3.4. Electroanalytical performance of the immunosensor

The manufacturing process of the immunosensor was characterized by EIS, DPV and SWV, respectively. As Fig. 2C, the resistance charge transfer (Rct) of bare GCE is 3929 Ω, which is reduced to 84.4 Ω after adsorption of PG-BP on the bare GCE surface, indicating a significant electron transfer kinetics between redox pairs. After the gold nanoparticles as a binding site of a cross-linking agent was bonded to the surface of the PG-BP, the Rct increased to 346.6 Ω, since the conductive capability of the gold nanoparticles was lower than that of PG-BP. However, when the AuNPs/PG-BP/GCE was laminated by semiconductor, the charge transfer resistance was remarkably lowered (Fig. 6S), which meant that the amino group was formed (Sonuc Karaboga et al., 2016). These amino terminals were protonated at this pH, which made the negatively charged redox probe readily diffuse onto the electrode surface. Thereafter, the Rct was significantly increased after the antibody immobilized on the electrode surface. This also demonstrated the successful formation of the anti-leptin layer on the surface of the modified electrode, which showed a blocking effect on the electron transfer kinetics. The final step was to inhibit the active Glu end by BSA, which also contributed a further increase in Rct. Comparing the results of Fig. 5S (DPV) and Fig. 2D (SWV) response curves, the response trend (enhanced or weakened) is consistent with the results expressed by the Nyquist plots, which fully supports the successful construction of electrochemical immunosensor (Fig. 2).

3.5. Analytical characteristics of the immunosensor

With the optimized conditions, the linear range of the prepared immunosensor was investigated. Voltammetry is a more sensitive and rapid analysis method than potentiometry and conductance. Among them, SWV technology is the most sensitive and superior one (Rizwan et al., 2018). Therefore, SWV was applied to analyze the performance of immunosensor in this study.

First, leptin was detected using BSA/anti-leptin/Glu/Cys/AuNPs/PG-BP/GCE. As shown in Fig. 4S, the current response of 0 pg/mL leptin-containing solution showed higher than that of 625 pg/mL leptin-containing solution. This is due to the fact that the strong negative charge on leptin is higher than its isoelectric point and hindrance in electron flow toward the electrode surface at pH 7.4, resulting in a reduction in the electrochemical signal.

To examine the analytical performance of this prepared immunosensor, different concentrations of leptin (0.15 pg/mL to 2500 pg/mL) was used as samples employing $[Fe(CN)_6]^{3-/4-}$ as electron mediator. The SWV was recorded at potential increment of 0.004 V and amplitude of 0.025 V with a frequency is 15 Hz. Fig. 3A is the dose-response curves of the immunosensors at different concentrations, ((a) 0.15 pg/mL, (b) 1 pg/mL, (c) 10 pg/mL, (d) 100 pg/mL, (e) 312 pg/mL, (f) 625 pg/mL, (g) 1250 pg/mL, (h) 2500 pg/mL) as the concentration of leptin increased, the corresponding signal decreased and eventually reached saturation. That is because more antigen-antibody immune complexes that served as an insulating layer and developed repulsive electrostatic

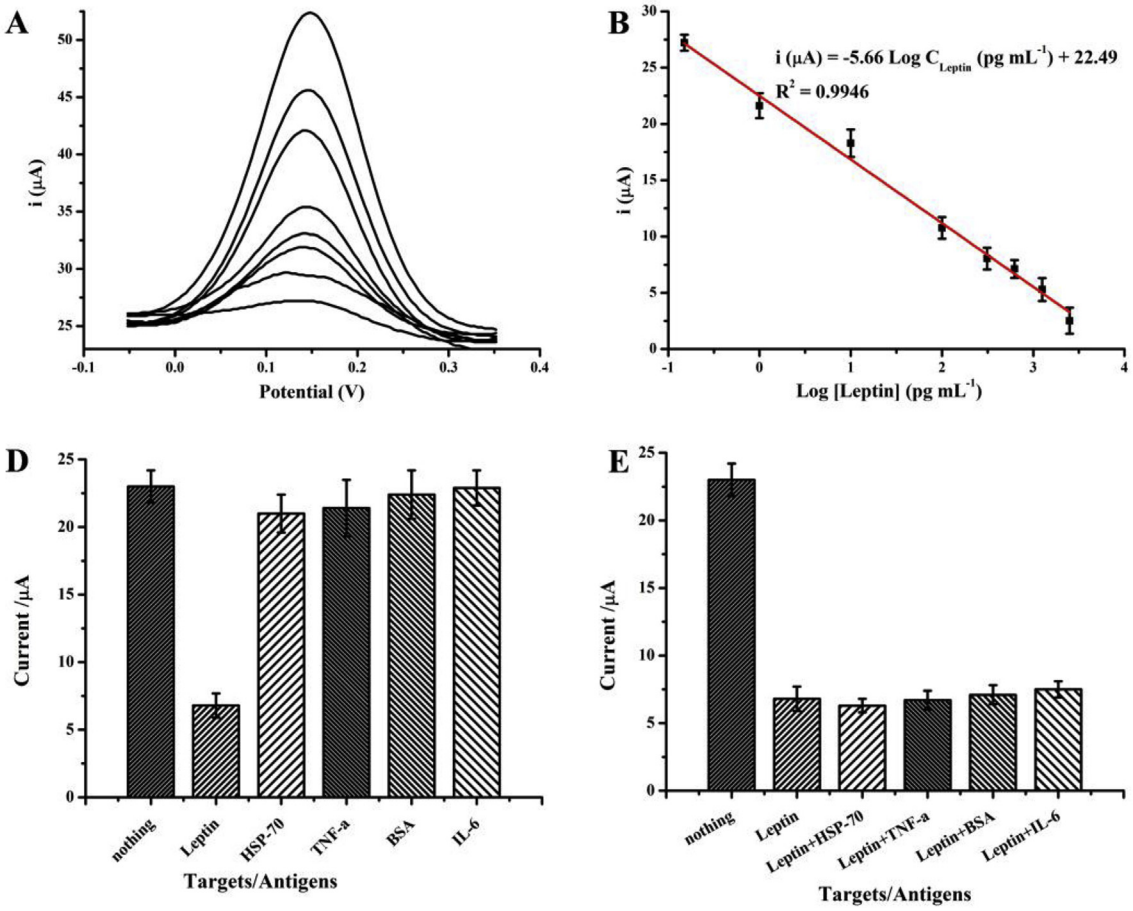

Fig. 3. (A) SWV response of the immunosensor to different concentrations of leptin (from a to h: 0.15, 1, 10, 100, 312, 625, 1250 and 2500 pg/mL). Measurements were performed in 0.5 mM $[Fe(CN)_6]^{3-/4-}$ solution in 0.1 M PBS (pH = 7.4); (B) Calibration curve based on the current reduction observed. (C) Selectivity of leptin-immunosensors, where 0 pg/mL leptin, 625 pg/mL leptin, and from bar shows the SWV peak current of 0 pg/mL leptin mixed with 625 pg/mL HSP-70, TNF-α, BSA and IL-6; (D) Interference-resistant of leptin-immunosensors, where 0 pg/mL leptin, 625 pg/mL leptin, and from bar shows the SWV peak current of 625 pg/mL leptin mixed with 100 ng/mL HSP-70, TNF-α, BSA and IL-6.

interaction between $[Fe(CN)_6]^{3-/4-}$ and antigen. As shown in Fig. 3A and B, there is a negative linear relationship between logarithm of leptin concentration and current from 0.15 pg/mL to 2500 pg/mL: i (μA) = −5.66 log C_{leptin} (pg/ml) + 22.49 and the correlation coefficient is 0.9946. Then, the limit of detection (LOD) was determined to be 0.036 pg/mL by calculating the average of the background signal generated by the matrix blank plus 3 times the mean standard deviation (3. Calculation of the limit of detection of supplemental material).

The high sensitivity of the leptin immunosensor can be attributed in part to the large surface area, low background current, and enhanced conductive capability of the PG-BP modified GCE platform. In addition, the good conductive capability, high biocompatibility and special cross-linking between AuNPs, Cys, Glu and biomolecules improved antibody immobilization, thereby the stability of the immunosensor was increased and the electrochemical signal of the immunosensor was amplified. Furthermore, $[Fe(CN)_6]^{3-/4-}$ is an excellent redox mediator in electrochemical systems that produces a steady current response with low background noise (Sonuc Karaboga et al., 2016).

Comparing with other reported human leptin assays, the prepared immunosensor showed better analytical performance and LOD (Table 1).

3.6. Selectivity, interference-resistant, reproducibility and stability

Due to the complex composition of biological samples, high selectivity and resistant to interference are necessary to immunosensors. In this study, HSP 70, tumor necrosis factor (TNF), BSA and interleukin-6 (IL-6) were used as interfering substances to evaluate the selectivity and correctly resistance to interference of the prepared immunosensor. Firstly, the selectivity of BSA/anti-leptin/Glu/Cys/AuNPs/PG-BP/GCE was evaluated by observing the electrochemical response of 0 pg/mL leptin, 625 pg/mL leptin and 625 pg/mL interferent (Fig. 3C). Secondly, the resistant to interference of BSA/anti-leptin/Glu/Cys/AuNPs/PG-BP/GCE was estimated by measuring the electrochemical response of 0 pg/mL leptin, 625 pg/mL leptin and 100 ng/mL interferent with 625 pg/mL leptin (Fig. 3D). It can be seen from Fig. 3C and D that the immunosensor constructed by the monoclonal anti-human leptin antibody has good selectivity and resistant to interference for the detection of human leptin.

The reproducibility of the immunosensor was assessed by repeating six replicates of the same leptin concentration (625 ng/mL), the relative standard deviation (RSD) between the measured values is 6.27%. This result indicates that the constructed immunosensor has acceptable reproducibility. At the same time, the prepared sensor was kept in a refrigerator from 0 to 7 days at 4 °C and tested with 625 ng/mL of leptin for stability study, and it can retain 92.32% of initial response after 7 days. The attenuation of the electrochemical response may be attributed to the gradual deactivation of biomolecules. In conclusion, the prepared immunosensor has acceptable stability for leptin detection.

Table 1
Comparison of different immunosensors for detection of leptin.

Linear range (pg/mL)	Detection limit (pg/mL)	Detection methods	References
1–800	0.3	Fe_3O_4/polydopamine/Au Nanocomposites electrode	He et al. (2015)
10–1000	1.9	hemin/G-quadruplex DNAzymes-assembled electrode	He et al. (2013)
50–500000	30	Carbon Nanotubes/Chitosan Film Modified Electrodes	Fang Dong (2014)
5–100	0.5	disposable electrochemical immunosensor	Ojeda et al. (2013)
0.78–50	0.78	ELISA	Imagawa et al. (1998)
0.15–2500	0.036	The proposed method	This sensor

Table 2
Real samples analysis (Human serum).

Dilution	Add conc. (pg/mL)	Found conc. (pg/mL)	RSD (%)	Recovery (%)
100 ×	100	98 ± 2.6	3.21	98 ± 2.6
	500	504 ± 4.2	1.43	100.8 ± 0.84
	1000	996 ± 3.2	5.2	99.6 ± 0.32

3.7. Real sample analysis

The feasibility of the label-free leptin immunosensor in practical applications was evaluated by detecting the leptin concentration in human serum. Human serum samples were diluted 100-fold with 10 mM PBS buffer and divided it into three shares, and then add three different concentrations of leptin (100, 500, 1000 pg/mL) for the electrochemical determination by recovery test, these results are summarized in Table 2. The RSD and the recovery of leptin in serum at 100, 500 and 1000 pg/mL are in the range of 1.43%–5.2% and 98 ± 2.6%–100.8 ± 0.84%, respectively. Therefore, the proposed immunosensor has significant potential for leptin detection in real serum samples.

4. Conclusion

In this study, a novel label-free immunosensor for detection of leptin in actual sample was developed. The base material PG-BP of the sensor exhibits strong electron transport behavior, and its effective specific surface area is also increased by about 5 times compared with bare GCE. The simple immobilization procedure of gold nanoparticles and the self-assembled layer of cysteamine make the antigen more firmly immobilized on the electrode surface. The proposed immunosensor displayed wide linear range (0.15–2500 pg/mL) and a low detection limit (0.036 pg/mL), which exhibits superior performance compared with the results of enzyme-linked immunosorbent assay and existing electrochemical methods. Therefore, this platform is expected to provide a reliable, real-time and convenient potential means for method for clinical trials of NAFLD markers.

CRediT authorship contribution statement

Jinying Cai: Supervision, Writing - review & editing. **Xiaodan Gou:** Writing - original draft. **Bolu Sun:** Formal analysis. **Wuyan Li:** Formal analysis. **Dai Li:** Formal analysis. **Jinglong Liu:** Investigation. **Fangdi Hu:** Conceptualization, Funding acquisition. **Yingdong Li:** Funding acquisition.

Acknowledgements

The authors acknowledge the National Key Research and Development Program of China (2018YFC1706300-3), Special funds for Innovation and Guidance of Gansu (2017ZX-02), the Science-Technology plan Project from Lanzhou Science and Technology Bureau (2016-2-80, 2017-4-119, 2017-RC115), the Key R&D Project of Gansu Provincial Science and Technology Department (17ZD2FA009), the National Traditional Chinese Medicine Standardization Project (ZYBZH-YGS-10), and the Key Project of the Fundamental Research Funds for the Central Universities (lzujbky-2018-k13, lzujbky-2017-205), and the project form Gansu Medical Products Administration.

Appendix A. Supplementary data

Supplementary data to this article can be found online at https://doi.org/10.1016/j.bios.2019.04.045.

References

Alkhouri, N., Tamimi, T.A., Yerian, L., Lopez, R., Zein, N.N., Feldstein, A.E., 2010. Dig. Dis. Sci. 55, 2644–2650.
Avsar, A., Veramarun, I.J., Tan, J.Y., Watanabe, K., Taniguchi, T., Castro Neto, A.H., Ozyilmaz, B., 2015. ACS Nano 9, 4138–4145.
Byrne, C.D., Targher, G., 2016. Diabetologia 59, 1141–1144.
Chalasani, N., Younossi, Z., Lavine, J.E., Charlton, M., Cusi, K., Rinella, M., Harrison, S.A., Brunt, E.M., Sanyal, A.J., 2012. Hepatology 55, 2005–2023.
Chen, Y., Ren, R., Pu, H., Chang, J., Mao, S., Chen, J., 2016. Biosens. Bioelectron. 89, 505–510.
Cho, I.H., Lee, J., Kim, J., Kang, M.S., Paik, J.K., Ku, S., Cho, H.M., Irudayaraj, J., Kim, D.H., 2018. Sensors-Basel 18.
Cho, S.Y., Lee, Y., Koh, H.J., Jung, H., Kim, J.S., Yoo, H.W., Kim, J., Jung, H.T., 2016. Adv. Meter. 28, 7020.
Fang Dong, R.L., Chen, Heng, Zhang, Wei, Ding, Shijia, 2014. Int. J. Eletrochem. Sc. 9, 6924–6935.
Gusmão, R., Sofer, Z., Pumera, M., 2017. Angew. Chem. Int. Ed. 56, 8052–8072.
He, Y., Sun, J., Wang, X., Wang, L., 2015. Sensor. Actuator. B Chem. 221, 792–798.
He, Y., Wang, X., Zhang, Y., Gao, F., Li, Y., Chen, H., Wang, L., 2013. Talanta 116, 816.
Imagawa, K., Matsumoto, Y., Numata, Y., Morita, A., Kikuoka, S., Tamaki, M., Higashikubo, C., Tsuji, T., Sasakura, K., Teraoka, H., 1998. Clin. Chem. 44, 2165–2171.
Jenkins, A.B., Markovic, T.P., Fleury, A., Campbell, L.V., 1997. Diabetologia 40, 348–351.
Kim, N., Son, S.H., 2016. J. Fluoresc. 26, 1715–1721.
Kumar, V., Brent, J.R., Shorie, M., Kaur, H., Chadha, G., Thomas, A.G., Lewis, E.A., Rooney, A.P., Nguyen, L., Zhong, X.L., Burke, M.G., Haigh, S.J., Walton, A., McNaughter, P.D., Tedstone, A.A., Savjani, N., Muryn, C.A., O'Brien, P., Ganguli, A.K., Lewis, D.J., Sabherwal, P., 2016. Acs. Appl. Mater. Inter. 8, 22860–22868.
Li, S., Lei, S., Yu, Q., Zou, L., Ye, B., 2018. Talanta 185, 453.
Liu, H., Tao, L., Zhang, Y., Xie, C., Zhou, P., Liu, H., Chen, R., Wang, S., 2017a. Acs. Appl. Mater. Inter. 9, 36849–36856.
Liu, H., Zou, Y., Tao, L., Ma, Z., Liu, D., Zhou, P., Liu, H., Wang, S., 2017b. Small 13, 1700758.
Liu, Y., Shang, T., Liu, Y., Liu, X., Xue, Z., Liu, X., 2018. Sensor. Actuator. B Chem. 263, 543–549.
Mayorga-Martinez, C.C., Mohamad Latiff, N., Eng, A.Y.S., Sofer, Z., Pumera, M., 2016. Anal. Chem. 88, 10074–10079.
Nong, J., Wei, W., Wang, W., Lan, G., Shang, Z., Yi, J., Tang, L., 2018. Optic Express 26, 1633–1644.
Ojeda, I., Moreno-Guzmán, M., González-Cortés, A., Yáñez-Sedeño, P., Pingarrón, J.M., 2013. Analyst 138, 4284–4291.
Pérez-Pérez, A., Vilariño-García, T., Fernández-Riejos, P., Martín-González, J., Segura-Egea, J.J., Sánchez-Margalet, V., 2017. Cytokine Growth Factor Rev. 35, 71–84.
Pang, Y., Jian, J., Tu, T., Yang, Z., Ling, J., Li, Y., Wang, X., Qiao, Y., Tian, H., Yang, Y., 2018. Biosens. Bioelectron. 116, 123–129.
Rau, M., Weiss, J., Geier, A., 2015. DMW (Dtsch. Med. Wochenschr.) 140, 1051–1055.
Rinella, M.E., Sanyal, A.J., 2016. Nat. Rev. Gastroenterol. Hepatol. 13, 196–205.
Rizwan, M., Elma, S., Lim, S.A., Ahmed, M.U., 2018. Biosens. Bioelectron. 107, 211–217.
Rui, G., Sofer, Z., Pumera, M., 2017. Angew. Chem. Int. Ed. 129, 8164–8185.
Rui, Z., Zhao, L., Liu, R., 2016. J. Photochem. Photobiol., B 163, 40–46.
Sajedimoghaddam, A., Mayorgamartinez, C.C., Sofer, Z., Bouša, D., Saievariranizad, E., Pumera, M., 2017. J. Phys. Chem. C 121, 20532–20538.

Schmidt, E.M.S., Escribano, D., Martinezsubiela, S., Martinezmiró, S., Hernández, F., Tvarijonaviciute, A., Cerón, J.J., Tecles, F., 2016. BMC Vet. Res. 12, 242.
Sonuc Karaboga, M.N., Simsek, C.S., Sezginturk, M.K., 2016. Biosens. Bioelectron. 84, 22–29.
Stannus, O.P., Cao, Y., Antony, B., Blizzard, L., Cicuttini, F., Jones, G., Ding, C., 2013. Ann. Rheum. Dis. 74, 82–88.
Sun, B., Cai, J., Li, W., Gou, X., Gou, Y., Li, D., Hu, F., 2018. Biosens. Bioelectron. 111, 34–40.
Tuteja, S.K., Neethirajan, S., 2018. Nanotechnology 29, 135101.
Wang, G.L., Yu, P.P., Xu, J.J., Chen, H.Y., 2009. J. Phys. Chem. C 113, 11142–11148.
Wen, W., Yan, X., Zhu, C., Du, D., Lin, Y., 2017. Sensors 17, 138–156.
Yáñezsedeño, P., Campuzano, S., Pingarrón, J.M., 2017. Sensors 17, 965–995.
Ye, L., Hu, Y., Xu, F.H., Cai, C.Y., Song, D.W., Xu, Z.S., Du, W.D., 2016. Proteonomics Clin. Appl. 11, 1600073.
Zhang, R., Gu, Y., Wang, Z., Li, Y., Fan, Q., Jia, Y., 2018. Biosens. Bioelectron. 117, 303–311.
Zhou, Y.Y., Zhou, X.D., Wu, S.J., Fan, D.H., Van, S.P., Chen, Y.P., Fu, S.W., Zheng, M.H., 2018. Hepatol. Commun. 2, 376–392.